

Heat transfer enhancement by perforated and louvred fins

Miftah Altwieb^{*1}, Rakesh Mishra², Aliyu M. Aliyu², Krzysztof J. Kubiak³

¹ *Department of Mechanical and Industrial Engineering, University of Gharyan, Libya*

² *School of Computing and Engineering, University of Huddersfield, United Kingdom*

³ *School of Mechanical Engineering, University of Leeds, United Kingdom*

Abstract

An experimental study was carried out to investigate the steady-state pressure drop and heat transfer characteristics of three multi-tube and fin heat exchangers. A comparison was made of the performance of a new perforated plain fin design with those of plain and louvred fins designs. Experimental test setups were designed for the three fin geometries and carefully assembled. Experiments were performed to quantify the heat transfer rate and pressure drop per unit length within these heat exchangers. The air velocity used in this study was in a range between 0.7 and 4 m/s. The water side flow rates in the tubes were 2, 3, 4, 5, and 6 L/min corresponding to a range of between 10000 and 30000 for the Reynolds number. It was found that for all inlet air velocities and water flow rates, the louvred fins produced the highest heat transfer rate due to the high available surface area; but it also produced the highest pressure drops when compared to the other two designs. Conversely, while the new perforated design produced a slightly higher pressure drop than the plain fin design, it gave a higher heat transfer rate than the plain fin especially at the lower liquid flow rates (of 2 and 3 L/min). The mean heat transfer rate and pressure drops has been then used to calculate the Colburn and Fanning friction factors respectively. Two new semi-empirical relationships were subsequently derived for the heat exchanger's Fanning friction factor and the Colburn factor as functions of the non-dimensional fin surface area and the Reynolds number. Furthermore, it was demonstrated that the Colburn and Fanning factors were predicted by the new correlations to within $\pm 15\%$ of the experimental data.

Keywords: heat exchanger, heat transfer, louvred fins, heat transfer effectiveness, Fanning friction factor, Colburn factor.

1 Introduction

The heat exchangers are devices used to transfer thermal energy between two or more mediums, which could be fluid–fluid or fluid–gas systems. In most heat exchangers, the heat transfer between the respective fluids is carried out through a separating wall and into a surrounding medium, and this can be a transient process. Hence, both convection and conduction are involved. Typical areas of heat exchanger application are processes with heating or cooling requirements of fluid streams, evaporation, or condensation. The heat

*Corresponding author email: a.m.aliyu@hud.ac.uk

exchangers are widely used in applications such as ventilation and air conditioning systems (HVAC), power generation and manufacturing system [1], [2].

There are specific guidelines and procedures for designing and predicting performance of the heat exchangers. Knowledge and adherence to these during a design process are of great importance for maintaining proper and efficient operation. Essentially, the procedures connect the overall heat transfer rate to numerous process or geometrical variables. The variables include flow arrangements, heat exchanger geometry, fins geometry, materials used, design specifications such as tube geometry, cost of operation and operating conditions.

In recent years, many studies have been carried out to analyse and to improve performance of the heat exchangers. The main aim of those studies is to enhance thermal performance of the heat exchangers while minimising pressure drop and reducing weight and cost. In general, optimisation approaches can be classified as active or passive techniques. In active techniques, an external force is used to drive heat transfer performance. Conversely, inserts and other additional geometrical protrusions are used to modify the flow in passive techniques. In practice however, a combination of both active and passive techniques may be used to increase the thermal and hydraulic performance of a fin and tube heat exchanger [3], [4].

Wilson [5] developed an experimental technique to measure and evaluate the convection coefficients in a number of convective heat transfer processes. The overall thermal resistance were divided into three major categories: internal convection, tube wall and external convection. The method has been extensively used and even adapted for use in modified systems i.e., for helical tubes and for pipe annuli. It assumes that the outside coefficient and the fouling resistance are constant and that the coefficients C_A , n_A , and m_A of the correlation devised are known:

$$Nu_A = C_A Re_A^{n_A} Pr_A^{m_A} \quad (1)$$

Modifications of the Wilson method were carried out by Sieder-Tate [6], Colburn [7] and Dittus-Boelter [8]. These modifications are mainly relating the Nusselt, Reynolds and Prandtl numbers in Equation (1).

Wang et al. [9] experimentally studied 15 plate, fin and tube heat exchangers with different geometries having a 3/8inch (9.52 mm) tube diameter. They examined the effect of fin thickness, fin spacing, number of tube rows and the heat transfer and friction characteristics showing that the fin thickness and spacing have no effect on the heat transfer or friction factor characteristics. Wang et al. also found that the number of tube rows has a negligible influence on a friction factor behaviour.

Abu Madi et al. [10] assessed the performance characteristics of finned plate and tube heat exchangers. They correlated geometry of flat and corrugated fins with Colburn and friction

factors. The fin type has an effect on heat transfer and friction factor. However, the number of tube rows is of much less significance. Furthermore, they found that the effect of the number of tube rows was influenced by the fin and tube geometries and the Reynolds number. According to Webb et al [11] and Wang et al [12], the most effective methods of enhancing the heat transfer performance is to extend the fin surface. Additionally, the plain fin is the most widely used due to its ease of manufacture, simplicity of assembly and has low pressure drop characteristics.

Wang et al. [13] analysed experimentally compact slit fins exchangers with plain and louvred fins. Similar to previous studies, a number of tube rows has small effect on the frictional performance. Louvred fins increased heat transfer.

Fernández-Seara et al. [14] adopted the Wilson plot method and designed an experimental apparatus to measure heat transfer coefficients in the processes of vapour generation and its condensation in heat exchanger tubes. They extended its use to a number of convection heat transfer problems which they noted will be useful to thermal design engineers.

Wang et al. [15] carried out an experimental study to compare the airside performance of plain, semi-dimpled vortex generator (VG) and louvred fin-and-tube heat exchangers. They investigated the effect of the number of tube rows and the effect of different fins on the heat transfer coefficient. Their results showed that number of tubes in a row has a negligible effect on the heat transfer coefficients for the louvred and semi-dimpled VG fin geometry. Moreover, the heat transfer coefficients for the louvred fin geometry were found to be about 2-15% higher than in the case of the semi-dimpled VG geometry. It is however noted that these findings are valid for heat exchangers with number of tubes rows of between 2 and 4.

Liu et al. [16] conducted CFD simulations to study the effect of perforation size, fin spacing, and number of perforations, on the Colburn factor of the air side. The heat transfer rates for finned-tube heat exchangers were also studied. Their results compared the heat transfer characteristics of the perforated and plain fins and they found that for constant fin spacing, the air-side Colburn factor increased by more than 3 and 8%, respectively when the air-side Reynolds number increases from 750 to 2350. Conversely, the perforated fins heat exchanger gave a higher air-side Colburn factor compared to the plain fins heat exchanger.

Kalantari et al. [17] carried out a parametric study over a wide range of design, geometrical and operating parameters. They investigated Reynolds numbers of up to 12,000 and found that longer fins, fin pitch and smaller tube diameter result in higher heat transfer coefficients. A correlation for the conjugate heat transfer coefficient was developed that applies to gas-liquid finned tube heat exchangers. In the correlation, the Nusselt number was expressed in terms of the Prandtl number and non-dimensional geometrical parameters.

Altwieb et al. [18] assessed the thermal performance of a multi-tube plain-finned heat exchanger with different geometrical modification using three-dimensional CFD simulations. Three enhancements were analysed: fin spacing, transverse pitch, and longitudinal pitch to determine their influence on the Colburn and Fanning factors. Validation experiments were carried out and compared with the CFD and were in turn utilised to calculate the Fanning and Colburn factors; and the local fin efficiency for each of the geometrical modifications. Two empirical correlations were developed for the Fanning and Colburn friction factors and the authors demonstrated predictions within 10% the experimental data. Similarly, Altwieb & Mishra [19] reported an experimental and numerical study on the response of multi tube and fin heat exchanger with plain, louvred and semi-dimple vortex generator. The heat transfer and pressure drop characteristics were investigated. Two new design equations were developed for the heat transfer rate and the pressure drop behaviour.

The scope of the work summarised above is quite limited since most investigations are focusing on the perforations of plain fins or are carried out using numerical simulations. Perforations are used to provide passive heat transfer enhancements in the heat exchanger. The effect of fin perforation on local and global performance indicators is a key and ongoing area of research that requires deeper understanding. Furthermore, the majority of equations developed for design purposes have limited applicability and do not include specific geometric parameters such as fin pitch, spacing, and the presence of perforations.

The aim of this paper is to experimentally investigate the steady state heat transfer and thermal performance of wide range of fin configurations (plain, louvred and perforated fin) heat exchanger. Using the experimental data, new semi-empirical prediction models for the Fanning friction factor (f) and Colburn factor (j) based on Reynolds number and heat exchanger geometry were developed and their prediction error margins analysed. It is envisaged that these equations will contribute to improve design and operation of such heat exchanger configurations.

2 Experiments

An experimental setup was designed and fabricated to study the steady-state thermal behaviour of a multi-tube and fin heat exchanger. Details of the setup, equipment, instrumentation, and uncertainties are given in the following sections.

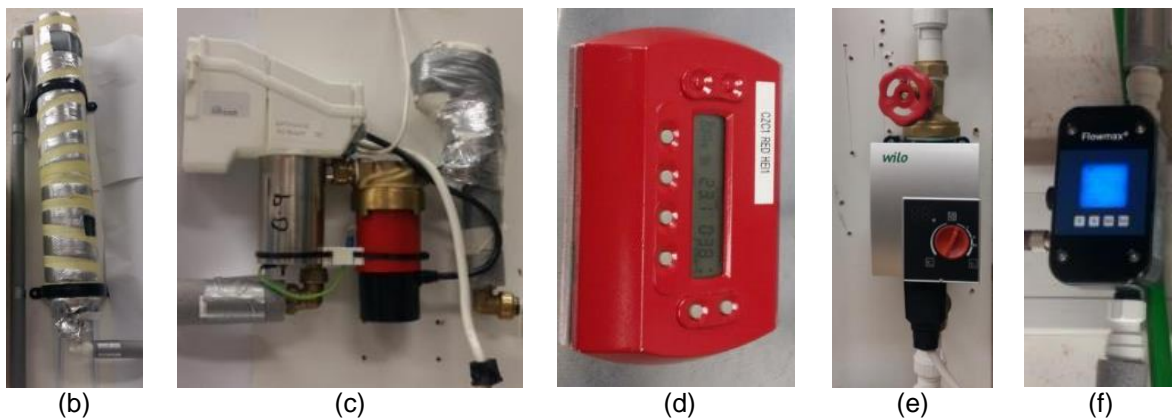
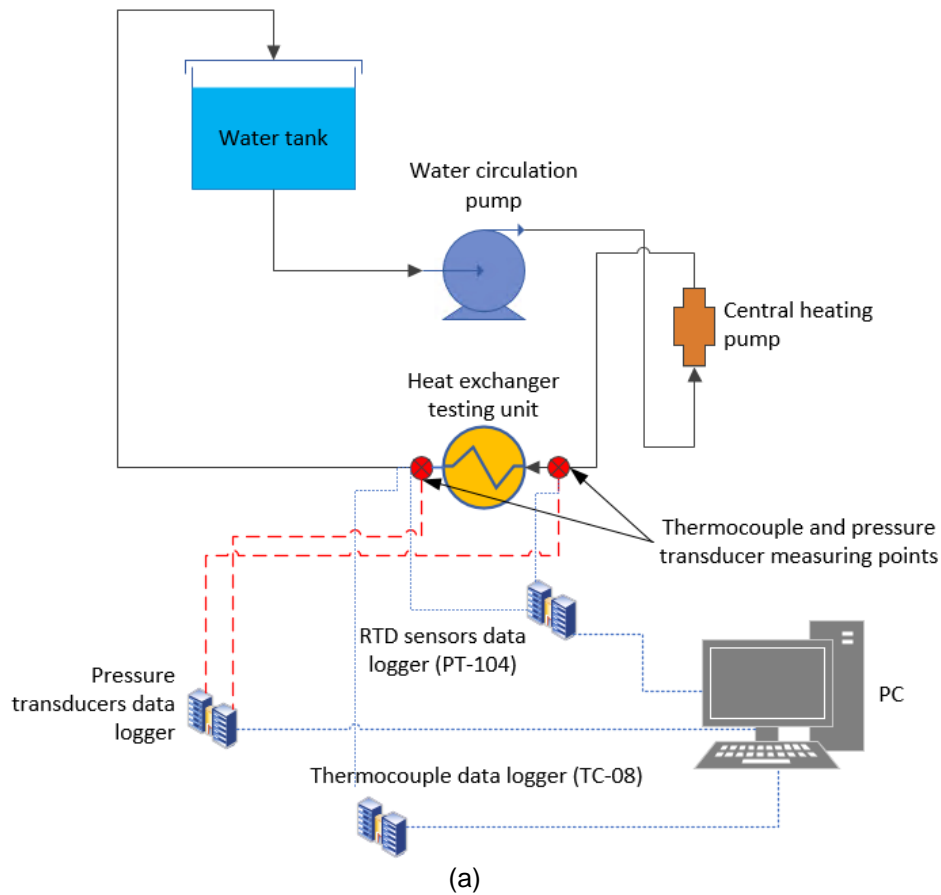


Figure 1: Schematic of the experimental setup: (a) overall schematic of a heater flow loop, (b) insulated 5 litre water tank, (c) water heater, (d) heater controller unit, (e) water pump, (f) water flow meter.

2.1 Experimental rig

The experimental setup is composed of the following parts: a 5-litre water tank (wrapped with a reflector foil to minimise heat loss), a heater, circulation pump integrated with a 0.9 kW heater unit, flow meter (Flowmax 44i with measuring range of 0.3–21 L/min), the heat exchanger testing unit, pressure transducers (IMP, with 0 – 10V analogue output signal and range 0–4 bars), T-type thermocouples (with accuracy of $\pm 0.15^{\circ}\text{C}$), thermocouples data logger, RTD sensors (PT100, with range of -75 – 250°C), RTD sensors data logger and a

personal computer for data acquisition. Figure 1 (a–f) is a schematic diagram of the experimental setup and photos of the various test rig components.

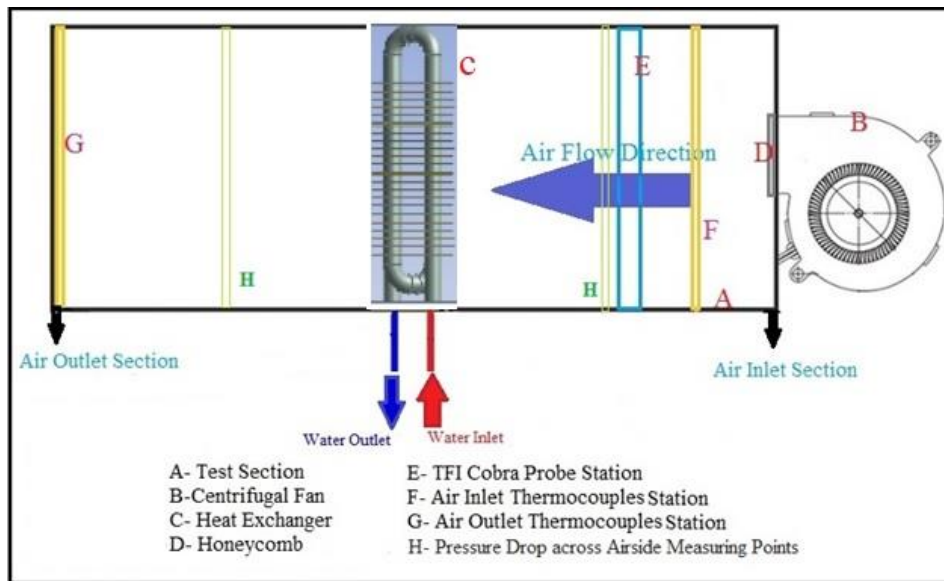
2.1.1 Heat Exchanger Testing Unit

Figure 2 (a) illustrates a schematic diagram of the heat exchanger testing unit. The testing unit was made from a 2-mm thick galvanised steel sheet. It has a length of 650 mm; a width of 165 mm and a height of 175 mm. Airflow is supplied to the testing unit using a single-sided centrifugal fan which has an incorporated Electronically Commutated (EC) motor. The fan has a power rating of 119 W and is able to deliver a maximum of 610 m³/h airflow rate. Speed of the fan's EC motor was controlled using a potentiometer.

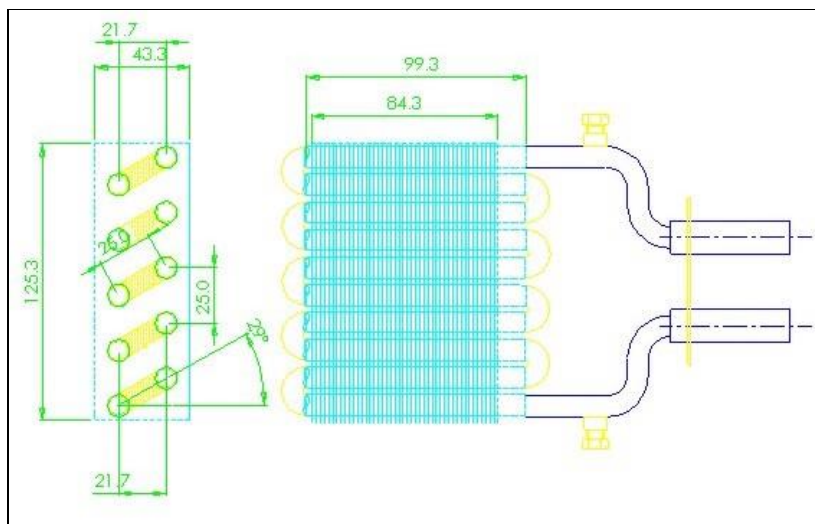
For suppressing the incoming free turbulence, a honeycomb structure was fitted at the centrifugal fan outlet (i.e., airflow inlet), it acts as a flow straightener. The inlet air velocity was measured by TFI cobra probe station as it enters the test section. The cobra probe is a multi-hole pressure sensor that is able to measure the incoming air velocity in all three directions. Furthermore, the ASHRAE standard 41.2 [15], [20] was applied to accurately measure the air velocity at twenty-five different points at the inlet section which were later averaged to obtain the mean air inlet velocity.

The upstream and downstream air temperatures within the testing unit were measured at two measuring stations. Each of the measuring stations consist of seven T-type thermocouples. The thermocouples have exposed welded copper/constantan tips to minimise its thermal inertia [15]. There are two main benefits of using seven thermocouples for each side. Firstly, the accuracy is improved since more samples are available for averaging. Secondly, automatic averaging is being carried out simultaneously for the inlet and outlet air temperature distributions at the measuring stations in both locations. The distribution of these thermocouples in the measuring station is shown in Figure 2 (c). During testing, the thermocouples were repeatedly checked and calibrated using a laboratory grade thermometer. All temperatures measured by the thermocouples were recorded using a Pico Technology (PicoTech) thermocouple data logger model TC-08. The data from the thermocouples were logged then averaged.

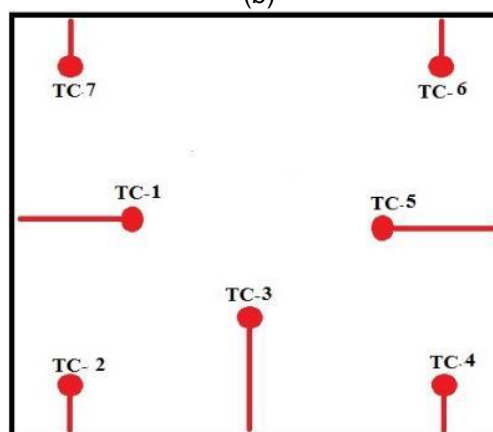
The inlet and outlet water temperatures in the tubes were measured by PicoTech temperature probes (RTD-PT100). The accuracy of these probes is $\pm 0.03^\circ\text{C}$ and during testing, the probes were repeatedly checked and calibrated using the thermometer. The water flow rate was metered using the Flowmax 44i water flowmeter which is an ultrasonic-based volumetric flow meter with a measurement range of 0.3–21 L/min. It has a $\pm 2\%$ maximum error of measurement and its repeatability is within $\pm 0.5\%$.



(a)



(b)



(c)

Figure 2: (a) Schematic of the heat exchanger testing unit, (b) dimensions of the plain fin heat exchanger, (c) Thermocouples distribution in the measuring station,

The heat exchanger's airside pressure drop was measured using a DPM TT550 micro-manometer. It has the ability of measuring the static pressure within the range: 0.4–5000 Pa.

The heat exchanger's water side pressure drop was measured using two pressure transducers. They were respectively placed at the water inlet and outlet tubes and were in turn connected to a PC via a USB-1616HS Series Data Acquisition interface. The voltage readings were then recorded and subsequently converted to a corresponding pressure using a previously determined calibration equation.

2.1.2 Fin geometries

Three main fin geometries were used to carry out this study. They are:

- a. Plain fin
- b. Perforated plain fin
- c. Louvred fin

The plain fin heat exchanger is a multi-tube and fin type. It consist of two tube rows, each with a diameter of 9.52 mm. Each row contains five 0.26-mm thick copper tubes, with the overall length of each tube being 130 mm. The bend of each tube has a diameter of 16 mm. The heat exchanger has 21 staggered 0.12 mm aluminium plain fins which have a width of 43.3 mm and a height 125.3 mm. Along the heat exchanger, the fins are placed at a distance of 4.23 mm from each other. The dimensions of the heat exchangers are shown in Figure 2 (b).

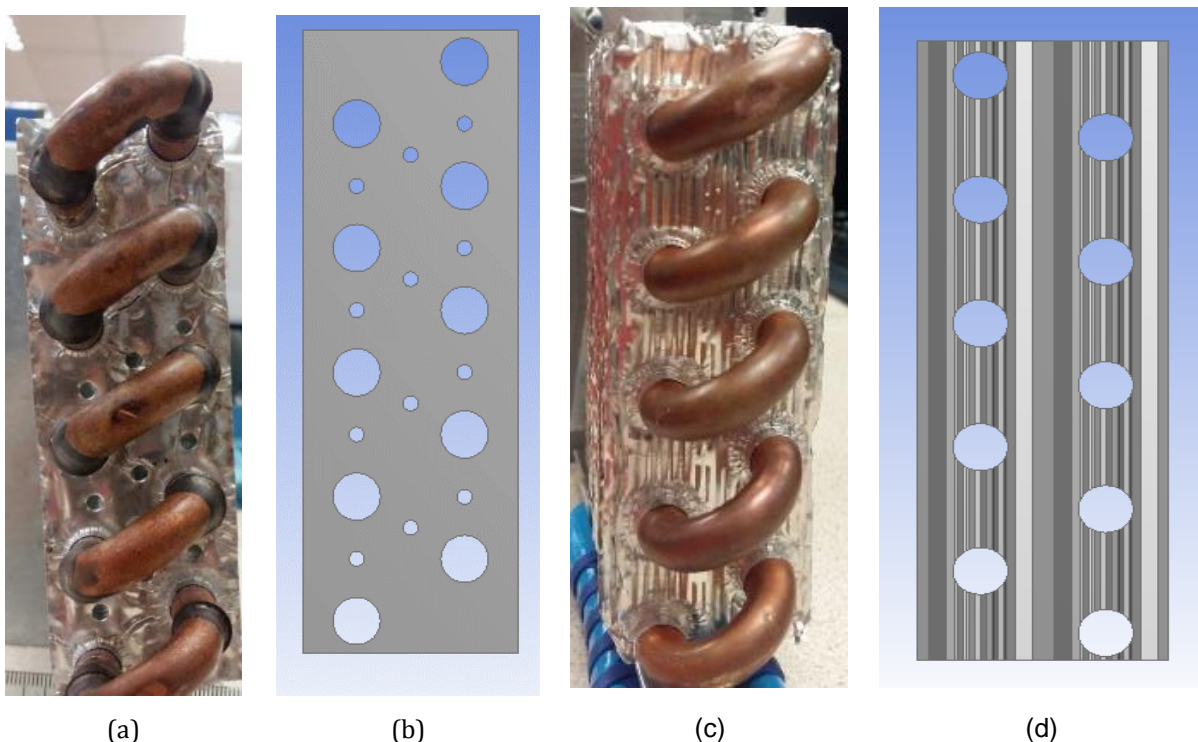


Figure 3: (a) Perforated plain fin heat exchanger, (b) perforated holes' distribution in fin geometry, (c) louvred fins heat exchanger, (d) louvred fin shape.

The perforated plain fins heat exchanger model was manufactured by punching twelve 3-mm diameter holes in each plain fin material. This is shown in Figure 3 (a and b) with the inclined

distribution of the 3-mm perforated holes. Finally, the louvred fins heat exchanger used has the same dimensions as the plain and perforated plain fin models. It is shown in Figure 3 (c) and is identical to the louvred fins used in Wang et al. [15].

2.1.3 Tests Procedure

Steady-state tests are the simplest to perform and evaluate since the flow is time independent. In the present study, tests were performed by drawing an airflow over the fins side of the heat exchanger, while circulating hot water through the tubes of the heat exchanger. The air velocity range used in this study is 0.7-4 m/s, which represents the arithmetic mean velocity of the gross cross-sectional area of the airflow (face area). The range for the water flow rate is 2–6 L/min, which makes the flow inside the tubes fully turbulent. The test matrix for the experiments carried out in this study are presented in Table 1. It shows that a total of 25 tests were carried out for 2 to 6 L/min water flow rate with 0.7-4 m/s air velocities for each water flow rate. Each test point was repeated twice to obtain a triplicate of measurements. An acceptable level of repeatability was obtained as measurements showed less than $\pm 3\%$ of deviation between each test conditions.

Table 1: Test matrix for the comparative steady-state tests conducted.

Test ID	Water Side		Air Side	
	Water Flow rate (L/min)	Water Inlet Temperature ($^{\circ}$ C)	Air Velocity (m/s)	Air Inlet Temperature ($^{\circ}$ C)
Test 1.1	2 \pm 0.03	60 \pm 1	0.705	24 \pm 1
Test 1.2			1.546	
Test 1.3			2.183	
Test 1.4			3.177	
Test 1.5			3.991	
Test 2.1	3 \pm 0.03	60 \pm 1	0.705	24 \pm 1
Test 2.2			1.546	
Test 2.3			2.183	
Test 2.4			3.177	
Test 2.5			3.991	
Test 3.1	4 \pm 0.03	60 \pm 1	0.705	24 \pm 1
Test 3.2			1.546	
Test 3.3			2.183	
Test 3.4			3.177	
Test 3.5			3.991	
Test 4.1	5 \pm 0.03	60 \pm 1	0.705	24 \pm 1
Test 4.2			1.546	
Test 4.3			2.183	
Test 4.4			3.177	
Test 4.5			3.991	
Test 5.1	6 \pm 0.03	60 \pm 1	0.705	24 \pm 1
Test 5.2			1.546	
Test 5.3			2.183	
Test 5.4			3.177	
Test 5.5			3.991	

2.2 Data Analysis

The temperatures of the hot water and air at the inlets and outlets as well as the respective pressure drops were measured. The heat transfer rate for water-side and air-side were then calculated as:

$$\dot{Q}_{hot} = m_w c_{pw} (T_{wi} - T_{wo}) \quad (2)$$

$$\dot{Q}_{cold} = m_a c_{pa} (T_{ao} - T_{ai}) \quad (3)$$

where the subscripts a and w indicate air and water; i and o indicate inlet and outlet respectively. The average heat transfer rate (\dot{Q}_{avg}) can be computed as follows:

$$\dot{Q}_{avg} = \frac{\dot{Q}_{hot} + \dot{Q}_{cold}}{2} \quad (4)$$

Furthermore, in order to carry out an assessment of a heat transfer and pressure drop characteristics, the Colburn factor (j) and Fanning friction factor (f) were calculated and used for this purpose. The f factor symbolises the pressure drop characteristics while the j factor symbolises the heat transfer characteristics and the j/f ratio is termed the efficiency index (j/f). The Colburn j factor and the friction factor f are respectively calculated using:

$$j = StPr^{2/3} \quad (5)$$

$$f = \frac{A_c \rho_m}{A_o \rho_1} \left[\frac{2\rho_1 \Delta P}{G_c^2} - (K_c + 1 - \sigma^2) - 2 \left(\frac{\rho_1}{\rho_2} - 1 \right) + (1 - \sigma^2 - K_e) \frac{\rho_1}{\rho_2} \right] \quad (6)$$

where A_c is the minimum free flow area of the air side; A_o is the total surface area of the air side; the variables K_c and K_e are the entrance and exit pressure loss coefficients. Equation (6) was proposed by Kays and London [21] using the data from Figures 14-26 in McQuiston et al. [2]. Additionally, the Stanton and the Prandtl numbers used to define the Colburn j -factor in Equation (5) are respectively given as:

$$St = \frac{h_o}{\rho_a V_{a(max)} c_{pa}} \quad (7)$$

$$Pr = \frac{\mu c_{pa}}{\lambda} \quad (8)$$

where h_o is the heat transfer coefficient based on the total surface area of the air side; ρ_a is the density of air, $V_{a(max)}$ is the maximum air velocity; c_{pa} is the specific heat capacity of air; μ and λ are the air dynamic viscosity and thermal conductivity respectively. Since the f and j factors are most commonly preferred by researchers to assess the performance of heat

exchanger fin strips, they will be used here for assessing the performance of the three geometries used in this study.

3 Results

In this section, the trends of the measured pressure drop, and heat transfer rates are studied and discussed in detail. They were used to calculate the j- and f-factors, and the efficiency index in order to characterise the performance of the three fin and tube heat exchanger models.

3.1 Performance comparison for

The plots in Figure 4 show the trend of the mean heat transfer rate (\dot{Q}_{avg}) when plotted with the air velocity for the three heat exchangers (i.e., with perforated plain fins, ordinary plain fins and louvred fins) over a range of water flow rates namely 2, 3, 4, 5 and 6 L/min. The error bars represent the combined uncertainty of the thermocouples and deviation between repeated measurements. The uncertainties were determined to be $\pm 5\%$.

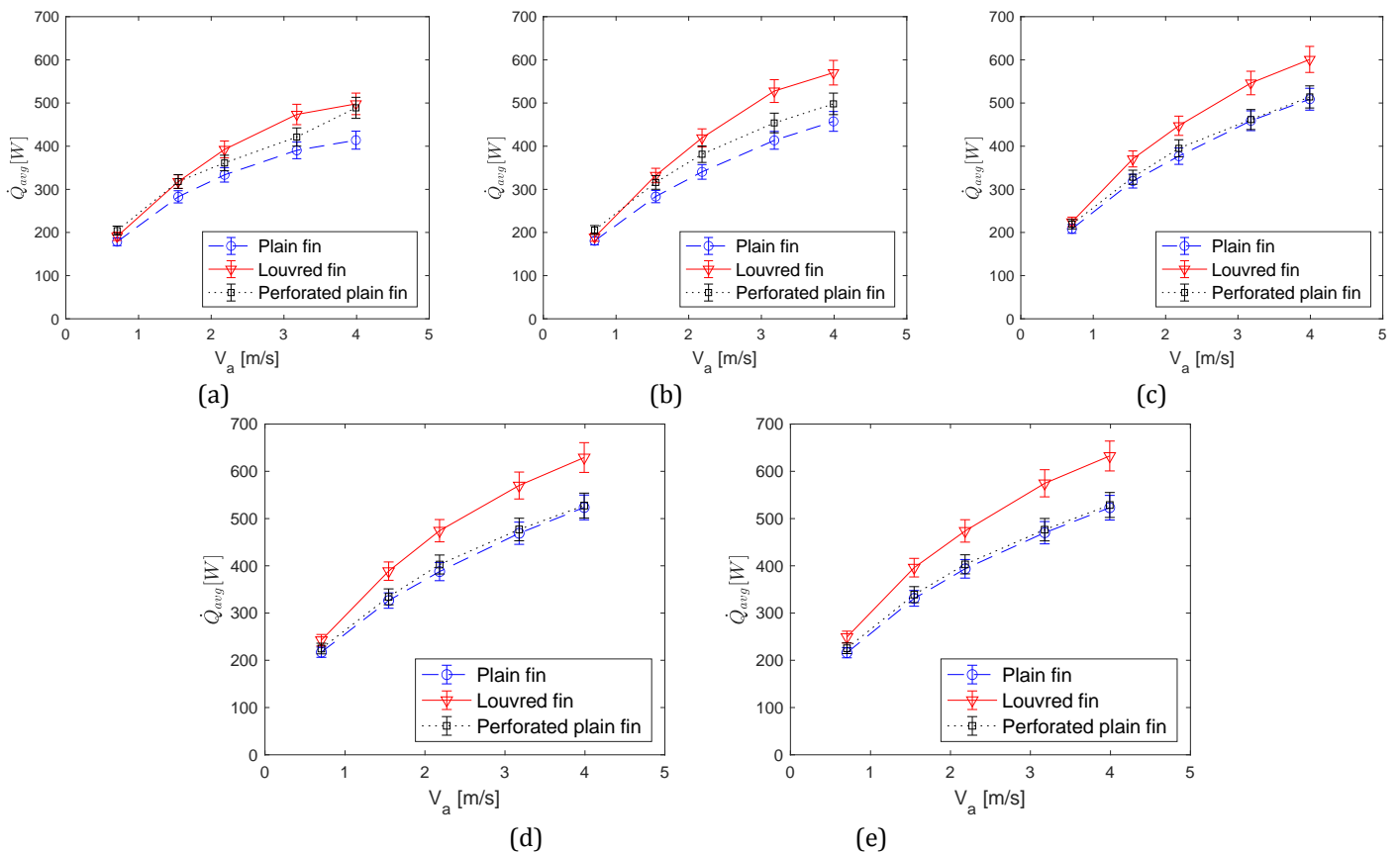


Figure 4 : Average heat transfer rate (\dot{Q}_{avg} [W]) against air velocity for the three heat exchangers with different fin arrangements and water flow rates; a) 2 L/min, b) 3 L/min, c) 4 L/min, d) 5 L/min and e) 6 L/min.

The plots in Figure 5 show the trend of pressure gradient across the airside of the heat exchanger against air velocity for the three heat exchanger geometries for water flow rates

ranging from 2 to 6 L/min. It can be seen from the figure that the louvred fins heat exchanger exhibited a higher mean heat transfer rate when compared with the perforated plain, and plain fins heat exchangers. For all cases, the pressure gradient increases as the water flow rate increases. However, the louvred fin geometry produced a linear proportionality as the air side velocity increases with an increasing slope at 5 and 6 L/min water flow rates. However, for the perforated and plain fin geometries, the increase in pressure gradient level off at 2 m/s air flow for all liquid flow rates.

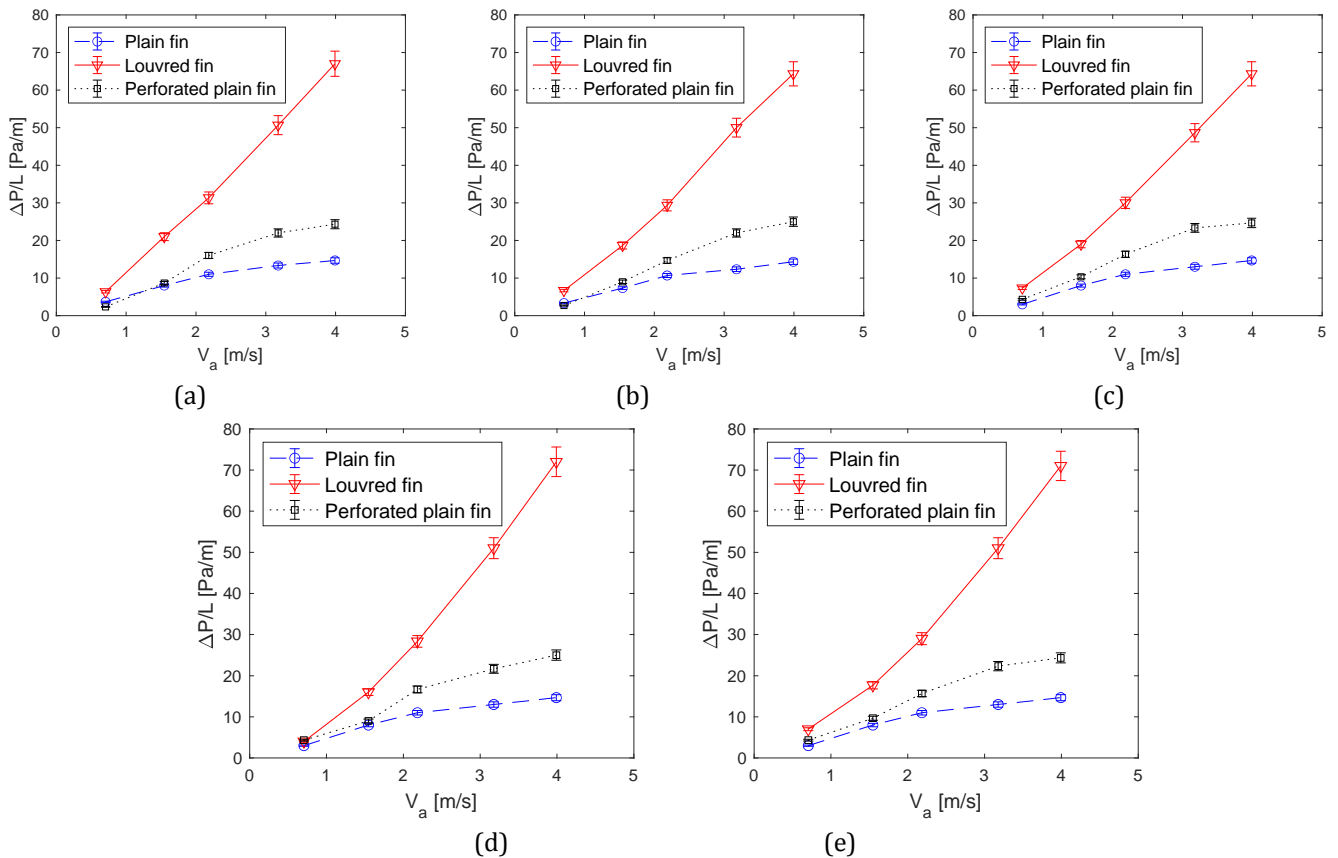
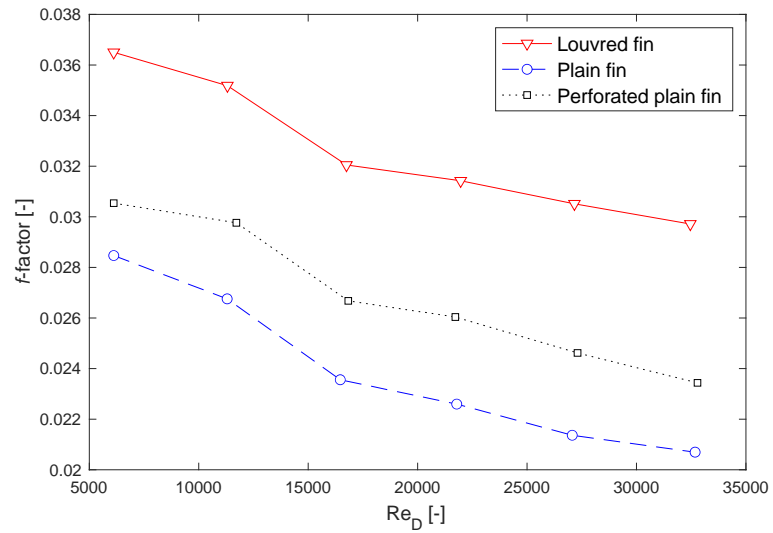
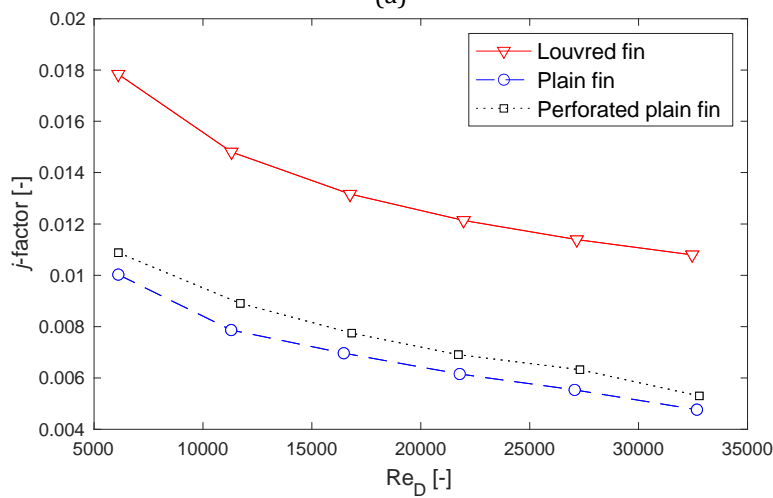


Figure 5: Variation of air side pressure gradient ($\Delta P/L$ [Pa/m]) against air velocity for three heat exchangers with different fin arrangements at various water flow rates; a) 2 L/min, b) 3 L/min, c) 4 L/min, d) 5 L/min and e) 6 L/min.

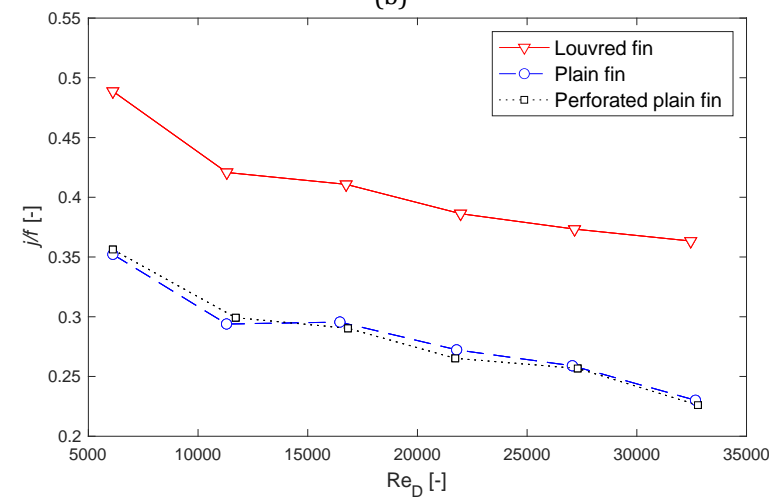
The louvred fins at flow rate of 4 L/min displayed the best average heat transfer rate with 16.95% and 14.15% increase when compared with the perforated and plain fins respectively. However, such significant increase of the heat transfer was made at the expense of a significant air pressure drop. The perforated fins increased the flow vorticity and also achieved increased heat transfer of 10.5% however, this effect is mainly visible for low water flow rates of 2 and 3 L/min. At 5 L/min the increase is only 3.65%.



(a)



(b)



(c)

Figure 6: Variations of (a) friction f -factor (b) Colburn j -factor and (c) efficiency index j/f for different fin arrangements as a function of Reynolds number.

Figure 6 (a) shows the variation of friction factor (f) for the heat exchangers as a function of Reynolds number. It shows that the friction factor decreases with increasing Reynolds number and is consistent with previous observations including those in the Moody chart for pipe flows.

For each of heat exchanger, there is a steep decreasing slope between $Re = 11000$ and 17000 before regaining more or less the same decreasing slope.

Figure 6 (b) depicts the variations of the Colburn j -factor the three heat exchangers as a function of Reynolds number. It shows that the Colburn j -factor decreases with increasing Reynolds number indicating a higher heat transfer rate at lower Reynolds numbers. The louvred fin heat exchanger gave the highest j values within the range 0.011 – 0.02 compared to 0.005 – 0.011 and 0.004 – 0.010 for the perforated and plain fin heat exchangers respectively. In similar fashion, Figure 6 (c) illustrates the variations of efficiency index (j/f) for three heat exchangers as a function of Reynolds number with an inverse relationship existing between the efficiency index and Re . While the louvred fin exhibits a far more superior efficiency than the other two geometries, the plain and perforated plain fin models gave near identical behaviour throughout the experimental range of Re investigated – with both geometries showing a similar efficiency index across the experimental range.

The plotted data in Figure 6 (a–c) reveals that, as the Reynolds number increases, the friction, Colburn factors and the efficiency index asymptotically decrease for all the three heat exchanger models. The high Colburn and friction factors for the louvred fins heat exchanger were observed when compared against the plain and perforated plain fin geometries. This can be explained as follows: as the surface area of the louvred fin is larger than that of the plain and perforated plain fin models. This fact results in an increase in the heat transfer coefficient which in turn leads to high Colburn j -factor values. However, the louvred fin heat exchanger's f -factor increased due to it increased surface area and a unique fin shape.

The results of heat transfer measurements showed an improvement in the average heat transfer rate (\dot{Q}_{avg}) of nearly 10% and 20% for the perforated plain fins and louvred fins heat exchangers respectively in comparison to the plain fins geometry. However, this improvement was accompanied by a 35% and 180% increase in pressure drop across the air-side respectively. The data for this study was used to develop two new empirical correlations for predicting the Fanning f - and Colburn j -factors as functions of the Reynolds number and the ratio of the fin total surface area to the total surface area of the heat exchanger available for heat transfer.

3.2 Development of new empirical relations for Fanning f and Colburn j -factor

The results obtained in the experimental campaign were used to develop a novel set of semi-empirical prediction models for the Fanning f - and the Colburn j -factors. As previously stated, the f - and j -factors quantify the pressure drop and heat transfer characteristics of the heat exchanger units. Therefore, it is imperative to develop correlations that relate them with the flow and geometrical parameters. The correlation procedure was carried out using multivariate

regression analysis using the curve fitting tools in Microsoft Excel's Solver ® and which are based on the least squares' method. The dimensionless geometric parameters used to develop the predictive correlation are the Reynolds number, Re_D and the ratio between total fin surface area to the total heat transfer surface area of the heat exchanger (A_f/A_t). Other authors have used similar dimensionless groupings to correlate the heat transfer properties of fin and tube heat exchangers [13], [17], [22]. The newly derived equations are as follows:

$$j = 10^{4.595} \left(A_f / A_t \right)^{29.918} Re_D^{-0.374} \quad (9)$$

$$f = 10^{1.203} \left(A_f / A_t \right)^{12.811} Re_D^{-0.139} \quad (10)$$

where Re_D is the Reynolds number based on the hydraulic diameter of the heat exchanger face's cross-section; D_c is fin collar outside diameter (m); A_f is the total surface area of the fins (m^2); A_t is the heat exchanger's overall heat transfer surface area (m^2). The equations ((9) and (10)) show that the Colburn and Fanning factors are inversely proportional to the Reynolds numbers which are consistent with experimental observations (in Figure 6 a and b). Additionally, the relatively large indices (29.218 and 12.811) for the (A_f/A_t) parameter reflects the relatively small magnitude of the fin area to the total heat transfer area. We caution that the equations should only be used for predicting the Fanning friction factor (f) and Colburn factors in multi-tube and fin heat exchangers with plain, louvered, and perforated fin arrangements. Furthermore, they should only be used at the Reynolds number range: $5 \times 10^3 \leq Re_D \leq 35 \times 10^3$ and for the heating cycle in forced convection heat transfer.

In order to graphically compare the performance Figure 7 (a) and (b) depict the relationship between the calculated values and the predicted values of Colburn factor (j) and Fanning friction factor (f), respectively. It can be seen that the percentage difference between the calculated and predicted values of the Colburn and Fanning factors are less than 15%. Furthermore, the correlation coefficient values between calculated and predicted data for Eqns. (9) and (10) are 0.853 and 0.811, respectively. Based on these, it may be concluded that the newly developed correlations show no significant difference to the collected experimental data, and they essentially exhibit the same trends.

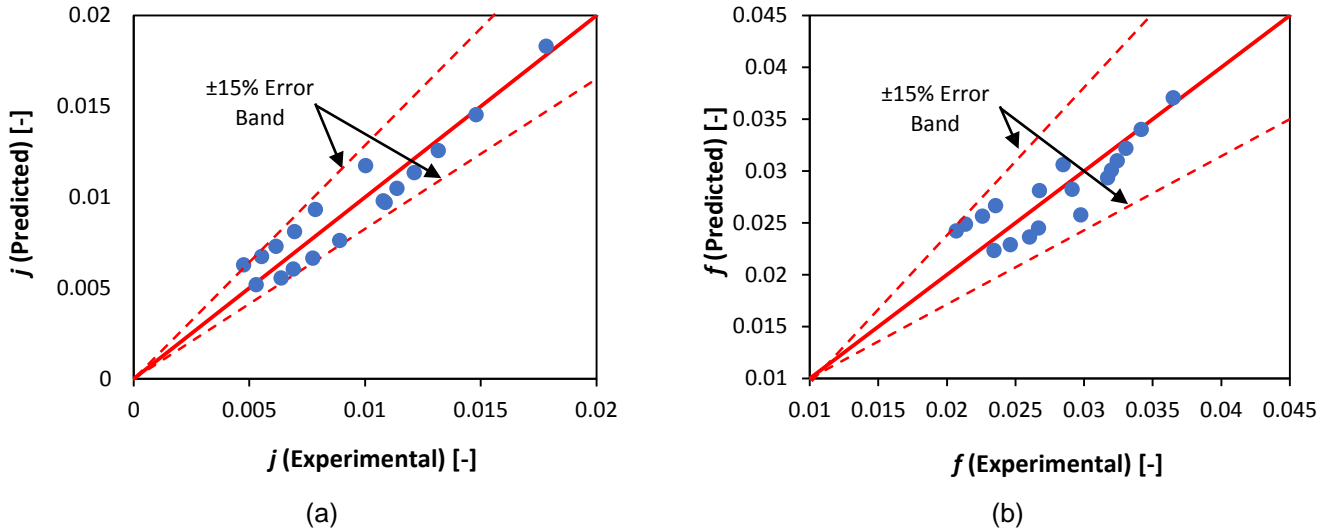


Figure 7: Comparisons of predicted (by Eqns. (9) and (10)) and experimental values of (a) Colburn j-factor and (b) Fanning f-factor

Therefore, it can be concluded that the developed equations are very much capable of predicting the Fanning f - and Colburn j -factors of these heat exchangers having the stated fin geometries with sufficient accuracy. Consequently, the equations can be used during the design and evaluation of existing multi-tube and fin heat exchanger with plain, perforated or louvered fins.

4 Conclusions

This study has presented novel geometric configurations for multi-tube and fin heat exchanger. The configurations were designed after conducting a robust experimental investigation with three heat exchanger geometries namely plain, perforated plain and louvered fin heat exchangers. Some important observations were made during the experiments and analysis of the pressure drop and heat transfer data. It was found that for all inlet air and water flow rates and hence velocities, the louvered fins produced the highest heat transfer rate. This was attributed to increased surface area available for heat transfer. Conversely, it also produced the highest pressure losses when compared to the other two designs. Also, while the new perforated design produced a slightly higher pressure drop than the plain fin design. Due to the vortices generated by the perforations, an enhancement in its heat transfer characteristics was observed when comparing with the plain and louvered fin models. This enhancement is relatively high at a small water flow rate. The experimental results were subsequently used to generate a set of empirical equations for design optimisation which can be used to predict the heat transfer and pressure drop characteristics of the heat exchangers represented by the Colburn and Fanning factors. The empirical equations were developed as functions of the heat exchangers' geometrical parameters, and we have shown that the performance of the equations are well within acceptable $\pm 15\%$ error margins in relation to the experimental data.

Funding

This research did not receive any external funding.

CRedit authorship contribution statement

M. Altwieb: Experimentation, Data curation, formal analysis, Investigation, methodology, validation, visualization, writing - original draft; **A. M. Aliyu:** Writing - review & editing, formal analysis; **K.J. Kubiak:** supervision, formal analysis, writing – review and editing; **R. Mishra:** Conceptualisation, supervision, writing – review and editing.

Declaration of Competing Interest

The authors declare no known competing financial interests or personal relationships that could have influence the work reported in this paper.

Nomenclature

Symbol	Description	Units
A_c	Flow cross sectional area	m^2
A_0	Surface area of air side	m^2
Cp_w	Specific heats for water	$J/kg K$
Cp_a	Specific heats for air	$J/kg K$
f	Fanning friction factor	
h_w	Heat transfer coefficient for water	$W/m^2 K$
h_a	Heat transfer coefficient for air	$W/m^2 K$
j	Colburn factor	
j/f	Efficiency index	
K_c	Entrance pressure-loss coefficient	
K_e	Exit pressure-loss coefficient	
\dot{m}_w	Mass flow rate for water	kg/sec
\dot{m}_a	Mass flow rate for air	kg/sec
Nu	Nusselt number	
Pr	Prandtl number	
ΔP	Pressure drop	Pa
\dot{Q}_h	Hot side heat transfer rate	W
\dot{Q}_c	Cold side heat transfer rate	W
\dot{Q}_{avg}	Average heat transfer rate	W
St	Stanton number	
Re_D	Reynolds number	

T_{wi}	Water inlet temperature	K
T_{wo}	Water outlet temperature	K
T_{ai}	Air inlet temperature	K
T_{ao}	Air outlet temperature	K

Greek symbols

δ_{wall}	Wall thickness	m
ε	Heat exchanger effectiveness	
η_f	Fin efficiency	%
ρ	Fluid density	kg/m³
ρ_a	Density of air	kg/m³
ρ_m	Mean density	kg/m³
σ	Ratio of the minimum flow area to the frontal area	
μ	Air dynamic viscosity	Ns/m²
λ	Thermal conductivity of wall material	W/m K

5 References

- [1] R. K. Shah and D. P. Sekulic, *Fundamentals of heat exchanger design*. John Wiley & Sons, 2003.
- [2] F. C. Mcquiston, J. D. Parker, and J. K. Spilter, *Heating, ventilating, and air conditioning: analysis and design*. Wiley, 2004.
- [3] P. Naphon and S. Wongwises, "A review of flow and heat transfer characteristics in curved tubes," *Renewable and Sustainable Energy Reviews*, vol. 10, no. 5, pp. 463–490, Oct. 2006, doi: 10.1016/J.RSER.2004.09.014.
- [4] K. Thulukkanam, *Heat Exchanger Design Handbook*, 2nd ed. Taylor & Francis, 2013.
- [5] E. E. Wilson, "A basis for rational design of heat transfer apparatus," *The J. Am. Soc. Mech. Engrs*, 1915, Accessed: Mar. 10, 2021. [Online]. Available: <https://ci.nii.ac.jp/naid/10003391952/>.
- [6] E. N. Sieder, G. E. TATE Foster Wheeler Corporation, and N. York, "Heat Transfer and Pressure Drop of Liquids in Tubes O Oil A, heating Oil B, heating Oil A, cooling Oil C, cooling," UTC, 2021. doi: 10.1021/IE50324A027.
- [7] A. P. Colburn, "A method of correlating forced convection heat-transfer data and a comparison with fluid friction," *International Journal of Heat and Mass Transfer*, vol. 7, no. 12, pp. 1359–1384, Dec. 1964, doi: 10.1016/0017-9310(64)90125-5.

- [8] F. W. Dittus and L. M. K. Boelter, "Heat transfer in automobile radiators of the tubular type," *International Communications in Heat and Mass Transfer*, vol. 12, no. 1, pp. 3–22, Jan. 1985, doi: 10.1016/0735-1933(85)90003-X.
- [9] C. C. Wang, Y. J. Chang, Y. C. Hsieh, and Y. T. Lin, "Sensible heat and friction characteristics of plate fin-and-tube heat exchangers having plane fins," *International Journal of Refrigeration*, 1996, doi: 10.1016/0140-7007(96)00021-7.
- [10] M. Abu Madi, R. A. Johns, and M. R. Heikal, "Performance characteristics correlation for round tube and plate finned heat exchangers," *International Journal of Refrigeration*, vol. 21, no. 7, pp. 507–517, Nov. 1998, doi: 10.1016/S0140-7007(98)00031-0.
- [11] R. L. Webb and N. H. Kim, "Advances in air-cooled heat exchanger technology," *Journal of Enhanced Heat Transfer*, vol. 14, no. 1, pp. 1–26, 2007, doi: 10.1615/JEnhHeatTransf.v14.i1.10.
- [12] C.-C. WANG, "A SURVEY OF RECENT PATENTS OF FIN-AND-TUBE HEAT EXCHANGERS FROM 2001 TO 2009," *International Journal of Air-Conditioning and Refrigeration*, vol. 18, no. 01, pp. 1–13, Mar. 2010, doi: 10.1142/s2010132510000022.
- [13] C. C. Wang, W. S. Lee, and W. J. Sheu, "A comparative study of compact enhanced fin-and-tube heat exchangers," *International Journal of Heat and Mass Transfer*, vol. 44, no. 18, pp. 3565–3573, Jul. 2001, doi: 10.1016/S0017-9310(01)00011-4.
- [14] J. Fernández-Seara, F. J. Uhía, J. Sieres, and A. Campo, "A general review of the Wilson plot method and its modifications to determine convection coefficients in heat exchange devices," *Applied Thermal Engineering*, vol. 27, no. 17–18, Pergamon, pp. 2745–2757, Dec. 01, 2007, doi: 10.1016/j.applthermaleng.2007.04.004.
- [15] C.-C. Wang, K.-Y. Chen, J.-S. Liaw, and C.-Y. Tseng, "An experimental study of the air-side performance of fin-and-tube heat exchangers having plain, louver, and semi-dimple vortex generator configuration," *International Journal of Heat and Mass Transfer*, vol. 80, pp. 281–287, Jan. 2015, doi: 10.1016/J.IJHEATMASSTRANSFER.2014.09.030.
- [16] X. Liu, J. Yu, and G. Yan, "A numerical study on the air-side heat transfer of perforated finned-tube heat exchangers with large fin pitches," *International Journal of Heat and Mass Transfer*, vol. 100, pp. 199–207, Sep. 2016, doi: 10.1016/j.ijheatmasstransfer.2016.04.081.
- [17] H. Kalantari, S. A. Ghoreishi-Madiseh, J. C. Kurnia, and A. P. Sasmito, "An analytical correlation for conjugate heat transfer in fin and tube heat exchangers," *International*

- Journal of Thermal Sciences*, vol. 164, p. 106915, Jun. 2021, doi: 10.1016/j.ijthermalsci.2021.106915.
- [18] M. Altwieb, K. J. Kubiak, A. M. Aliyu, and R. Mishra, "A new three-dimensional CFD model for efficiency optimisation of fluid-to-air multi-fin heat exchanger," *Thermal Science and Engineering Progress*, vol. 19, Oct. 2020, doi: 10.1016/j.tsep.2020.100658.
- [19] M. O. Altwieb and R. Mishra, "Experimental and Numerical Investigations on the Response of a Multi Tubes and Fins Heat Exchanger under Steady State Operating Conditions," in *6th International and 43rd National Conference on Fluid Mechanics and Fluid Power*, 2016, pp. 1–3, [Online]. Available: <http://eprints.hud.ac.uk/id/eprint/29556/>.
- [20] C. C. Wang, K. Y. Chen, and Y. T. Lin, "Investigation of the semi-dimple vortex generator applicable to fin-and-tube heat exchangers," *Applied Thermal Engineering*, vol. 88, pp. 192–197, Sep. 2015, doi: 10.1016/j.applthermaleng.2014.09.054.
- [21] W. M. Kays and A. L. London, *Compact heat exchangers*. New York: Hemisphere Publishing, 1984.
- [22] Z. M. Lin, L. B. Wang, and Y. H. Zhang, "Numerical study on heat transfer enhancement of circular tube bank fin heat exchanger with interrupted annular groove fin," *Applied Thermal Engineering*, vol. 73, no. 2, pp. 1465–1476, 2014, doi: 10.1016/j.applthermaleng.2014.05.073.